Supplement of Hydrol. Earth Syst. Sci., 24, 4463–4489, 2020
https://doi.org/10.5194/hess-24-4463-2020-supplement

Hydrology and Earth System Sciences
Open Access
EGU

Supplement of

A systematic assessment of uncertainties in large-scale soil loss estimation from different representations of USLE input factors – a case study for Kenya and Uganda

Christoph Schürz et al.

Correspondence to: Christoph Schürz (christoph.schuerz@boku.ac.at) and Mathew Herrnegger (mathew.herrnegger@boku.ac.at)

Supplementary materials for the manuscript: *'A systematic assessment of uncertainties in large scale soil loss estimation from different representations of USLE input factors - A case study for Kenya and Uganda'*

This supplementary document provides additional detail on the generation of the USLE model inputs and the data sources that were used for their calculation. Further, the analysis steps and additional results are included here.

Contents

S.1 USLE model input factors - Definitions and equations

The following tables provide an overview of the methods that were implemented to generate the USLE input factor realizations shown in the work-flow in Fig. 2 of the main document. The tables below provide the names of the input realizations as they were used in the main document, the regarding equations and definitions to compute the respective input realizations and references of primary sources and studies that implemented the respective methods.

S.1.1 Rainfall erosivity R

Table S.1 shows the nine realizations for the R factor that were used in the study. The first six methods that were implemented relate R to the annual precipitation P_{annual}. In all cases P_{annual} was calculated from long-term monthly mean precipitations derived from the WordClim V2 data base (Fick and Hijmans, 2017) that were summarized to annual average sums. The realization $R_{Fenta,MFI}$ employed the Modified Fournier Index (MFI; Arnoldus, 1980), that was calculated from the long-term monthly precipitation sums derived from the WordClim V2 data base. The realizations R_{TMPA} and $R_{GloREDa}$ are large scale rainfall erosivity products available upon request from Vrieling et al. (2014) and Panagos et al. (2017), respectively.

Table S.1: Methods to calculate the rainfall erosivity factor R

Realization	Definition	References
R_{Roose}	$R = 0.5 \cdot P_{annual} \cdot 17.3$, (value 17.3 conversion factor from imperial to SI units)	Roose (1975), Morgan (2009)
R_{Moore}	$KE_{15} = 11.46 \cdot P_{annual} - 2226$, $R = 0.0029 \cdot KE - 26.0$, $R_{SI} = 17.02 \cdot R$	Moore (1979)
R_{Lo}	$R = 3.48 \cdot P_{annual} + 38.46$	Lo et al. (1985), Karamage et al. (2017)
R_{Renard}	$R = 0.0483 \cdot P_{annual}^{1.61}, P_{annual} \leq 850mm$, $R = 587.8 - 1.219 \cdot P_{annual} + 0.004105 \cdot P_{annual}, P_{annual} \geq 850mm$	Renard and Freimund (1994), Ferro et al. (1991), Yu and Rosewell (1996), Naipal et al. (2015), Yang et al. (2003)
R_{Nakil}	$R = 839.15 \cdot e^{P_{annual}}$	Nakil (2014)
$R_{Fenta,P}$	$R = 4.5 \cdot P_{annual} - 661.3$	Fenta et al. (2017), Fenta et al. (2020)
$R_{Fenta,MFI}$	$MFI = \sum_{i=1}^{i=12} \frac{p_i^2}{P_{annual}}$, $R = 27.8 \cdot MFI - 189.2$	Arnoldus (1980), Fenta et al. (2017), Fenta et al. (2020)
R_{TMPA}	R estimates for Africa derived from 3-hourly rainfall TRMM-TMPA data with 0.25-degree spatial resolution employing the procedure described in Renard and Freimund (1994)	Vrieling et al. (2014)
$R_{GloREDa}$	R estimates from 3540 stations records worldwide, using RBF and multiple global input features for global interpolation on a 1km grid	Panagos et al. (2017)

S.1.2 Soil erodibility K

To calculate spatial estimates of the Soil erodibility *K* two global soil data products were implemented SoilGrids250m (Hengl et al., 2017) and the Global Soil Dataset for use in Earth System Models (GSDE, Shangguan et al., 2014). From both products layers of sand, silt, and clay fractions, organic carbon content and coarse soil fractions/rock fragments were acquired for the first 10cm and weighted averages over the depths were calculated. Soilgrids250m additionally provides a soil classification layer according to the World Reference Base (WRB) that was used to derive the soil structure.

Table S.2 gives an overview of the six realizations for *K* that were used in this study. More detail on the equations of the methods are given in in table S.14. The soil structure and soil permeability classifications that were required to compute *K* employing the method of Wischmeier and Smith (1987) as described in Panagos et al. (2014) are listed in the tables S.4 and S.5.

Table S.2: Methods to calculate soil erodibility K

Realization	Definition	References
$K_{SoilGrids,Wischmeier}$	Mean values of sand, silt, and clay fractions for the soil depths 0 - 10cm derived from SoilGrids250m layers employed in the equation of Wischmeier and Smith (1987) and applying the corrections described in Panagos et al. (2014) (additionally employing the coarse fractions layer from SoilGrids250m). The soil structure s was derived from the World Reference Base (WRB) soil classification layer available from SoilGrids250m and a corresponding structure classification based on Baruth et al. (2006) as described in Panagos et al. (2014) or Borrelli et al. (2017)	Panagos et al. (2014), Panagos et al. (2015c), Borrelli et al. (2017)
$K_{SoilGrids,Williams}$	Mean values of sand, silt, clay, and organic carbon percentages for the soil depths 0 - 10cm derived from SoilGrids250m layers employed in the equation of Williams (1995)	Karamage et al. (2017), Yang et al. (2003)
$K_{SoilGrids,Torri}$	Mean values of sand, silt, clay, and organic carbon fractions for the soil depths 0 - 10cm derived from SoilGrids250m layers employed in the equation of Torri et al. (1997)	Yang et al. (2003), Naipal et al. (2015), Torri et al. (1997)
$K_{GSDE,Wischmeier}$	Mean values of sand, silt, and clay fractions for the soil depths 0 - 10cm derived from SoilGrids250m layers employed in the equation of Wischmeier and Smith (1987) and applying the corrections described in Panagos et al. (2014) (additionally employing the coarse fractions layer from GSDE). The soil structure s and permeability p were set to 2 and 3 as default values, respectively, as shown in Tamene and Le (2015)	Tamene and Le (2015)

Realization	Definition	References
$K_{GSDE,Williams}$	Mean values of sand, silt, and clay fractions for the soil depths 0 - 10cm derived from GSDE layers employed in the equation of Williams (1995)	Yang et al. (2003)
$K_{GSDE,Torri}$	Mean values of sand, silt, clay, and organic carbon fractions for the soil depths 0 - 10cm derived from GSDE layers employed in the equation of Torri et al. (1997)	Yang et al. (2003), Naipal et al. (2015), Torri et al. (1997)

Table S.14 provides the equations for the three implemented methods of Wischmeier and Smith (1987), Williams (1995), and Torri et al. (1997). The inputs that are required in the respective methods to compute K are the mass fractions (in percent) of Sand m_{Sand}, Silt m_{Silt}, Clay m_{Clay}, and organic matter/carbon content $orgC$.

Table S.3: Summary of the K factor realizations

Author	Equations
Wischmeier and Smith (1987)	$K = 0.1317 \cdot \frac{0.00021 \cdot M^{1.14} \cdot (12 - orgC) + 3.25 \cdot (s-2) + 2.5 \cdot (p-3)}{100}$, $M = (m_{Silt} + m_{vfSand}) * (100 - m_{Clay})$
Williams (1995)	$K = 0.1317 \cdot f_{cSand} \cdot f_{Cl-Si} \cdot f_{orgC} \cdot f_{hiSand}$, $f_{cSand} = 0.2 \cdot 0.3e^{-0.0256 \cdot m_{Sa} \cdot (1 - \frac{m_{Silt}}{100})}$, $f_{Cl-Si} = \frac{m_{Silt}}{m_{Clay} + m_{Silt}}$, $f_{orgC} = 1 - \frac{0.0256 \cdot orgC}{orgC + e^{3.72 - 2.95 \cdot orgC}}$, $f_{hiSand} = 1 - \frac{0.7 \cdot SN}{SN + e^{-5.51 + 22.9 \cdot SN}}$, $SN = 1 - \frac{m_{Sand}}{100}$
Torri et al. (1997)	$0.0293 \cdot (0.65 - D_g + 0.24 \cdot D_g^2) \cdot f_{orgC,Clay}$, $D_g = 0.01 \cdot (-3.5 \cdot m_{Sand} - 2.0 \cdot m_{Silt} - 0.5 \cdot m_{Clay})$, $f_{orgC,Clay} = e^{-0.0021 \cdot \frac{orgC}{m_{Clay}/100} - 0.00037 \cdot (\frac{orgC}{m_{Clay}/100})^2 - 4.02 \cdot \frac{m_{Clay}}{100} + 1.71 \cdot (\frac{m_{Clay}}{100})^2}$

Table S.4: Lookup table to derive the soil structure s from the soil taxonomy classification according to WRB

WRB value	Soil name	Qualifier	Soil group	Structure class s
1	Haplic Acrisols	Haplic	AC	2
2	Haplic Acrisols (Alumic)	Haplic	AC	2
3	Haplic Acrisols (Ferric)	Haplic	AC	2
4	Haplic Acrisols (Humic)	Haplic	AC	4
5	Plinthic Acrisols	Plinthic	AC	2
6	Vetic Acrisols	Vetic	AC	2
7	Haplic Albeluvisols	Haplic	AB	2
8	Histic Albeluvisols	Histic	AB	2
9	Umbric Albeluvisols	Umbric	AB	2
10	Cutanic Alisols	Cutanic	AL	2

WRB value	Soil name	Qualifier	Soil group	Structure class s
11	Haplic Alisols	Haplic	AL	2
12	Aluandic Andosols	Aluandic	AN	1
13	Haplic Andosols	Haplic	AN	1
14	Vitric Andosols	Vitric	AN	1
15	Albic Arenosols	Albic	AR	2
16	Ferralic Arenosols	Ferralic	AR	2
17	Haplic Arenosols	Haplic	AR	2
18	Haplic Arenosols (Calcaric)	Haplic	AR	2
19	Hypoluvic Arenosols	Hypoluvic	AR	2
20	Protic Arenosols	Protic	AR	2
21	Haplic Calcisols	Haplic	CL	2
22	Haplic Calcisols (Sodic)	Haplic	CL	2
23	Luvic Calcisols	Luvic	CL	2
24	Petric Calcisols	Petric	CL	2
25	Endogleyic Cambisols	Endogleyic	CM	4
26	Ferralic Cambisols	Ferralic	CM	2
27	Haplic Cambisols	Haplic	CM	2
28	Haplic Cambisols (Calcaric)	Haplic	CM	1
29	Haplic Cambisols (Chromic)	Haplic	CM	1
30	Haplic Cambisols (Dystric)	Haplic	CM	1
31	Haplic Cambisols (Eutric)	Haplic	CM	1
32	Haplic Cambisols (Humic)	Haplic	CM	4
33	Haplic Cambisols (Sodic)	Haplic	CM	1
34	Leptic Cambisols	Leptic	CM	1
35	Vertic Cambisols	Vertic	CM	1
36	Calcic Chernozems	Calcic	CH	2
37	Haplic Chernozems	Haplic	CH	2
38	Luvic Chernozems	Luvic	CH	2
39	Haplic Cryosols	Haplic	CR	2
40	Turbic Cryosols	Turbic	CR	2
41	Vitric Cryosols	Vitric	CR	2
42	Petric Durisols	Petric	DU	2
43	Acric Ferralsols	Acric	FR	2
44	Haplic Ferralsols	Haplic	FR	2
45	Haplic Ferralsols (Rhodic)	Haplic	FR	2
46	Haplic Ferralsols (Xanthic)	Haplic	FR	2
47	Umbric Ferralsols	Umbric	FR	2
48	Haplic Fluvisols	Haplic	FL	2
49	Haplic Fluvisols (Arenic)	Haplic	FL	2
50	Haplic Fluvisols (Calcaric)	Haplic	FL	2
51	Haplic Fluvisols (Dystric)	Haplic	FL	2
52	Haplic Fluvisols (Eutric)	Haplic	FL	2
53	Calcic Gleysols	Calcic	GL	2
54	Haplic Gleysols	Haplic	GL	2
55	Haplic Gleysols (Dystric)	Haplic	GL	2

WRB value	Soil name	Qualifier	Soil group	Structure class s
56	Haplic Gleysols (Eutric)	Haplic	GL	2
57	Mollic Gleysols	Mollic	GL	4
58	Umbric Gleysols	Umbric	GL	2
59	Calcic Gypsisols	Calcic	GY	2
60	Haplic Gypsisols	Haplic	GY	2
61	Calcic Histosols	Calcic	HS	4
62	Cryic Histosols	Cryic	HS	4
63	Fibric Histosols	Fibric	HS	4
64	Hemic Histosols	Hemic	HS	4
65	Sapric Histosols	Sapric	HS	4
66	Calcic Kastanozems	Calcic	KS	2
67	Haplic Kastanozems	Haplic	KS	2
68	Haplic Leptosols	Haplic	LP	2
69	Haplic Leptosols (Eutric)	Haplic	LP	2
70	Lithic Leptosols	Lithic	LP	2
71	Mollic Leptosols	Mollic	LP	2
72	Rendzic Leptosols	Rendzic	LP	4
73	Haplic Lixisols	Haplic	LX	2
74	Haplic Lixisols (Chromic)	Haplic	LX	2
75	Haplic Lixisols (Ferric)	Haplic	LX	2
76	Albic Luvisols	Albic	LV	2
77	Calcic Luvisols	Calcic	LV	2
78	Gleyic Luvisols	Gleyic	LV	2
79	Haplic Luvisols	Haplic	LV	2
80	Haplic Luvisols (Chromic)	Haplic	LV	2
81	Haplic Luvisols (Ferric)	Haplic	LV	2
82	Leptic Luvisols	Leptic	LV	2
83	Stagnic Luvisols	Stagnic	LV	2
84	Vertic Luvisols	Vertic	LV	2
85	Alic Nitisols	Alic	NT	2
86	Haplic Nitisols (Rhodic)	Haplic	NT	1
87	Haplic Phaeozems	Haplic	PH	1
88	Leptic Phaeozems	Leptic	PH	2
89	Luvic Phaeozems	Luvic	PH	4
90	Endogleyic Planosols	Endogleyic	PL	2
91	Haplic Planosols (Dystric)	Haplic	PL	2
92	Haplic Planosols (Eutric)	Haplic	PL	2
93	Luvic Planosols	Luvic	PL	2
94	Solodic Planosols	Solodic	PL	2
95	Acric Plinthosols	Acric	PT	2
96	Lixic Plinthosols	Lixic	PT	2
97	Gleyic Podzols	Gleyic	PZ	2
98	Haplic Podzols	Haplic	PZ	2
99	Aric Regosols	Aric	RG	2
100	Calcaric Regosols	Calcaric	RG	2
101	Haplic Regosols (Dystric)	Haplic	RG	2

WRB value	Soil name	Qualifier	Soil group	Structure class s
102	Haplic Regosols (Eutric)	Haplic	RG	2
103	Haplic Regosols (Sodic)	Haplic	RG	2
104	Leptic Regosols	Leptic	RG	2
105	Gypsic Solonchaks	Gypsic	SC	2
106	Haplic Solonchaks	Haplic	SC	2
107	Haplic Solonchaks (Sodic)	Haplic	SC	2
108	Calcic Solonetz	Calcic	SN	2
109	Gleyic Solonetz	Gleyic	SN	2
110	Haplic Solonetz	Haplic	SN	2
111	Mollic Solonetz	Mollic	SN	1
112	Luvic Stagnosols	Luvic	ST	4
113	Haplic Umbrisols	Haplic	UM	4
114	Leptic Umbrisols	Leptic	UM	1
115	Calcic Vertisols	Calcic	VR	2
116	Haplic Vertisols	Haplic	VR	2
117	Haplic Vertisols (Eutric)	Haplic	VR	2
118	Mollic Vertisols	Mollic	VR	2

Table S.5: Lookup table to derive the soil permeability p from the USDA soil texture classification

Value	USDA texture class	Permeability class p
1	Clay	6
2	Silty Clay	6
3	Sandy Clay	5
4	Silty Clay Loam	5
5	Clay Loam	4
6	Sandy Clay Loam	4
7	Silt	3
8	Silty Loam	3
9	Loam	3
10	Sandy Loam	2
11	Loamy Sand	2
12	Sand	1

S.1.3 Slope length and slope steepness LS

The calculation of the *LS* factor was based on two global elevation products the SRTM90m V4.1 (Jarvis et al., 2008) and the ASTER GDEM V4 (NASA/METI/AIST/Japan Spacesystems, and U.S./Japan ASTER Science Team, 2009) with a spatial resolution of 30m. Computational limitations required a resampling of the ASTER 30m DEM to the extent of the 90m grid of SRTM90m V4.1. Corrections of the input layers as recommended and performed in Panagos et al. (2015a) were considered for both input DEM layers.

Both input layers were pre-processed and prepared for the computation of *LS*. A DEM fill

and the flow direction calculation was performed according to Wang and Liu (2006). Flow accumulation and contributing catchment areas were calculated with the methods of Freeman (1991) and Quinn et al. (1991). Spatial slope estimates for both DEM products were calculated with the method of Zevenbergen and Thorne (1987). The pre-processing of the input DEM layers was done in ArcGIS 10.2 (ESRI, 2012).

To compute the *LS* factor realizations the methods of Moore et al. (1991), Desmet and Govers (1996), and Böhner and Selige (2006) were applied using the pre-processed layers based on SRTM90m and ASTER GDEM. For details to the methods we refer to the respective literature and will not repeat the methods' equations here. All implemented methods are available from the LS calculation module in SAGA GIS V2.1.4 (Conrad et al., 2015). Table S.6 gives an overview of the six realizations for *K* that were used in this study.

Table S.6: Summary of the LS factor realizations

Realization	Definition	References
$LS_{SRTM,Moore}$	Slope and Catchment Area derived from SRTM90m V4.1 implemented in the method of Moore et al. (1991)	Bosco et al. (2015)
$LS_{SRTM,Desmet}$	Slope and Catchment Area derived from SRTM90m V4.1 implemented in the method of Desmet and Govers (1996)	Borrelli et al. (2017)
$LS_{SRTM,Boehner}$	Slope and Catchment Area derived from SRTM90m V4.1 implemented in the method of Böhner and Selige (2006)	-
$LS_{ASTER,Moore}$	Slope and Catchment Area derived from ASTER GDEM V4 implemented in the method of Moore et al. (1991)	Bosco et al. (2015)
$LS_{ASTER,Desmet}$	Slope and Catchment Area derived from ASTER GDEM V4 implemented in the method of Desmet and Govers (1996)	Karamage et al. (2017), Borrelli et al. (2017)
$LS_{ASTER,Boehner}$	Slope and Catchment Area derived from ASTER GDEM V4 implemented in the method of Böhner and Selige (2006)	-

S.1.4 Crop cover management C

To compute the *C* we applied two different approaches. One approach estimates the C-factor from vegetation indices that are readily available from satellite based remote sensing. The majority of applications in literature that we found utilized the normalized difference vegetation index (NDVI) to assess *C* (e.g. Karamage et al., 2017; Naipal et al., 2015) and applied the method proposed by Van der Knijff et al. (2000):

$$C = \exp\left(-\alpha \frac{NDVI}{\beta - NDVI}\right)$$

with $\alpha = 1$ and $\beta = 2$, involving different temporal aggregates of the MODIS NDVI (Didan, 2015). MODIS NDVI provides 16 day averages. Spatially distributed mean NDVI estimates were calculated on annual basis and for the rainy season based on the 16 day averages for the time period 2000 to 2012. These mean NDVI estimates were used in the equation above to compute two spatially distributed realizations of the *C* factor.

The second approach relates land uses classified in land cover products and agricultural statistics to *C* values derived from field experiments (e.g. Borrelli et al., 2017; Panagos et al., 2015b; Yang et al., 2003). Two agricultural statistics products were implemented, a global product of spatially distributed crop shares provided by Monfreda et al. (2008) and agricultural surveys in Kenya and Uganda (KNBS, 2015; UBOS, 2010). In their global study Borrelli et al. (2017) grouped the crops available from Monfreda et al. (2008) and assigned *C* factor literature values. We used the same crop grouping that is summarized in table S.7. We employed *C* factor literature values that were available from Borrelli et al. (2017), Panagos et al. (2015b), Angima et al. (2003). Table S.8 shows the *C* factor literature values for specific crop groups adapted from Borrelli et al. (2017) that were used in this study.

Table S.7: Grouping of crops available from Monfreda et al. (2008) based on Borrelli et al. (2017)

Group ID	Crop	Label
11	Manila fibre (abaca)	abaca
11	Agave fibres nes	agave
8.2	Forage and silage, alfalfa	alfalfa
14	Almonds, with shell	almond
7	Anise, badian, fennel, coriander	aniseetc
14	Apples	apple
14	Apricots	apricot
14	Areca nuts	areca
4	Artichokes	artichoke
6	Asparagus	asparagus
14	Avocados	avocado
2	Bambara beans	bambara
14	Bananas	banana
1	Barley	barley
2	Beans, dry	bean
3	Beets for fodder	beetfor
12	Berries nes	berrynes
12	Blueberries	blueberry
14	Brazil nuts, with shell	brazil
2	Broad beans, horse beans, dry	broadbean
1	Buckwheat	buckwheat
7	Cabbages and other brassicas	cabbage
7	Cabbage for fodder	cabbagefor
10	Canary seed	canaryseed
14	Carobs	carob
3	Carrots and turnips	carrot
3	Carrots for fodder	carrotfor
14	Cashew nuts, with shell	cashew
14	Cashew apple	cashewapple
3	Cassava	cassava
10	Castor oil seed	castor
7	Cauliflowers and broccoli	cauliflower

Group ID	Crop	Label
1	Cereals, nes	cerealnes
14	Cherries	cherry
14	Chestnut	chestnut
2	Chick peas	chickpea
3	Chicory roots	chicory
4	Chillies and peppers, green	chilleetc
13.1	Cinnamon (canella)	cinnamon
14	Fruit, citrus nes	citrusnes
13.1	Cloves	clove
8.1	Forage and silage, clover	clover
14	Cocoa, beans	cocoa
14	Coconuts	coconut
13.2	Coffee, green	coffee
11	Coir	coir
10.1	Seed cotton	cotton
2	Cow peas, dry	cowpea
12	Cranberries	cranberry
5	Cucumbers and gherkins	cucumberetc
12	Currants	currant
14	Dates	date
4	Eggplants (aubergines)	eggplant
11	Fibre crops nes	fibrenes
14	Figs	fig
11	Flax fibre and tow	flax
1	Fonio	fonio
8.2	Forage products	fornes
14	Fruit, fresh nes	fruitnes
6	Garlic	garlic
3	Ginger	ginger
12	Gooseberries	gooseberry
9.1	Grapes	grape
14	Grapefruit (inc. pomelos)	grapefruitetc
8.1	Forage and silage, grasses nes	grassnes
2	Beans, green	greenbean
2	Leguminous vegetables, nes	greenbroadbean
1.1	Maize, green	greencorn
6	Onions, shallots, green	greenonion
2	Peas, green	greenpea
2	Groundnuts, with shell	groundnut
14	Gums	gums
14	Hazelnuts, with shell	hazelnut
13.1	Hemp tow waste	hemp
13.1	Hempseed	hempseed
9.2	Hops	hop
11	Jute	jute
11	Bastfibres, other	jutelikefiber

Group ID	Crop	Label
11	Kapok fibre	kapokfiber
14	Kapok fruit	kapokseed
14	Karite nuts (sheanuts)	karite
14	Kiwi fruit	kiwi
14	Kola nuts	kolanut
8.1	Forage and silage, legumes	legumenes
14	Lemons and limes	lemonlime
2	Lentils	lentil
7	Lettuce and chicory	lettuce
10	Linseed	linseed
2	Lupins	lupin
1.1	Maize	maize
8.1	Forage and silage, maize	maizefor
14	Mangoes, mangosteens, guavas	mango
13.1	Maté	mate
5	Melons, other (inc.cantaloupes)	melonetc
5	Melonseed	melonseed
1	Millet	millet
1	Mixed grain	mixedgrain
10	Mustard seed	mustard
13.1	Nutmeg, mace and cardamoms	nutmeg
14	Nuts, nes	nutnes
1	Oats	oats
14	Oil, palm fruit	oilpalm
8.2	Forage and silage, green oilseeds	oilseedfor
10	Oilseeds nes	oilseednes
4	Okra	okra
14	Olives	olive
6	Onions, dry	onion
14	Oranges	orange
14	Papayas	papaya
2	Peas, dry	pea
14	Peaches and nectarines	peachetc
14	Pears	pear
4	Pepper (piper spp.)	pepper
13.1	Peppermint	peppermint
14	Persimmons	persimmon
2	Pigeon peas	pigeonpea
4	Chillies and peppers, dry	pimento
14	Pineapples	pineapple
14	Pistachios	pistachio
14	Plantains	plantain
14	Plums and sloes	plum
1.1	Popcorn	popcorn
10	Poppy seed	poppy
3	Potatoes	potato

Group ID	Crop	Label
2	Pulses, nes	pulsenes
5	Pumpkins, squash and gourds	pumpkinetc
13.1	Pyrethrum, dried	pyrethrum
14	Quinces	quince
7	Quinoa	quinoa
13.1	Ramie	ramie
10	Rapeseed	rapeseed
12	Raspberries	rasberry
1.2	Rice, paddy	rice
3	Roots and tubers, nes	rootnes
14	Rubber, natural	rubber
1	Rye	rye
8.2	Forage and silage, rye grass	ryefor
10	Safflower seed	safflower
10	Sesame seed	sesame
11	Sisal	sisal
1	Sorghum	sorghum
8.2	Forage and silage, sorghum	sorghumfor
14	Cherry sour	sourcherry
2	Soybeans	soybean
13.1	Spices, nes	spicenes
7	Spinach	spinach
14	Fruit, stone nes	stonefruitnes
12.1	Strawberries	strawberry
2	String beans	stringbean
3	Sugar beet	sugarbeet
13.1	Sugar cane	sugarcane
13.1	Sugar crops, nes	sugarnes
10	Sunflower seed	sunflower
3	Swedes for fodder	swedefor
3	Sweet potatoes	sweetpotato
14	Tangerines, mandarins, clementines, satsumas	tangetc
3	Taro (cocoyam)	taro
13.1	Tea (0.1-0.2)	tea
7.1	Tobacco, unmanufactured	tobacco
4	Tomatoes	tomato
1	Triticale	triticale
14	Fruit, tropical fresh nes	tropicalnes
14	Tung nuts	tung
3	Turnips for fodder	turnipfor
13.1	Vanilla	vanilla
7	Vegetables, fresh nes	vegetablenes
3	Vegetables and roots fodder	vegfor
2	Vetches	vetch
14	Walnuts, with shell	walnut

Group ID	Crop	Label
5	Watermelons	watermelon
1	Wheat	wheat
3	Yams	yam
3	Yautia (cocoyam)	yautia
8.2	Mixed grass	mixedgrass
4	Mushrooms	mushroom

Table S.8: C factor literature values for specific crop groups based on Borrelli et al. (2017)

Group ID	Crop group	Label	C
1	Cereal Grains	cereal	0.2
1.1	Maize	maize	0.38
1.2	Rice	rice	0.15
2	Legume Vegetables	veg_legume	0.32
3	Root and Tuber Vegetables	veg_root	0.34
4	Fruit Vegetables	veg_fruit	0.25
5	Cucurbit Vegetables	veg_cucurbit	0.25
6	Bulb Vegetables	veg_bulb	0.3
7	Leafy Vegetables	veg_leaf	0.25
7.1	Tobacco	tobacco	0.5
8.1	Mixed Legumes	for_legume	0.15
8.2	Mixed grasses	for_grass	0.1
9.1	Grapes	grape	0.35
9.2	Hops	hop	0.42
10	Oilseed Group	oilseed	0.25
10.1	Cotton	cotton	0.4
11	Fibre Crops	fibre	0.28
12	Berries Group	berry	0.15
12.1	Strawberries	strawberry	0.2
13.1	Shrubs Herbs and Spices	herb_spice	0.15
13.2	Coffee	coffee	0.2
14	Trees/Fruit Tree	tree	0.15

Implementing the approach of Panagos2015, we calculated spatially distributed weighted average C-factor values for agricultural areas in the study domain based on the crop shares that were available from Monfreda et al. (2008) and the national agricultural surveys:

$$C_{(x,y)} = \sum_{i=1}^{n} C_i \cdot fraction_{i,(x,y)}$$

where $C_{(x,y)}$ is the weighted C-factor for the location (x, y), C_i is the C-factor of the crop i, n is the total number of crops, and $fraction_{i,(x,y)}$ is the calculated fraction of the area cultivated with crop i at the location (x, y).

The calculated average C values according to the crop shares were superimposed with the two land cover products MODIS Land Cover (Channan et al., 2014) and ESA CCI LC (ESA, 2017). To combination of MODIS land cover with C values for agricultural land uses was performed as described in Panagos et al. (2015b). C values of non agricultural land uses were derived from Panagos et al. (2015b) and Borrelli et al. (2017) for MODIS LC. Panagos et al. (2015b) propose ranges of C values for natural vegetation land uses and calculate the C value in a location based on the vegetation density derived from MODIS VCF. For the ESA CCI LC product average C values for non agricultural land uses were calculated based on the shares of a land cover described in the ESA CCI LC legend and the ranges of C values proposed by Panagos et al. (2015b), similar to MODIS LC and MODIS VCF. The combination of C factor values of crops and non agricultural land uses was performed accordingly:

$$C_{(x,y)} = C_{Crop,(x,y)} \cdot w_{Crop,(x,y)} + C_{LC,(x,y)} \cdot w_{LC,(x,y)}$$

where $C_{Crop,(x,y)}$ and $C_{LC,(x,y)}$ are the C values of the crop and the non agricultural land cover for the location (x, y) and $w_{Crop,(x,y)}$ and $w_{LC,(x,y)}$ are the respective weights values of the crop and the non agricultural land cover for the location (x, y). The respective non agricultural C factor values and weights for MODIS LC and ESA CCI LC can be found in the tables S.9 and S.10.

Table S.9: MODIS land cover classification linked with C factor ranges of the respective land cover and weights to calculate mixed C values for shared landuses of non crop land cover and crops

Value	*Label*	C_{min}	C_{max}	w_{Crop}	w_{LC}
0	Water	-	-	0	1
1	Evergreen Needleleaf forest	0.0001	0.003	0	1
2	Evergreen Broadleaf forest	0.0001	0.003	0	1
3	Deciduous Needleleaf forest	0.0001	0.003	0	1
4	Deciduous Breoadleaf forest	0.0001	0.003	0	1
5	Mixed forest	0.0001	0.003	0	1
6	Closed shrublands	0.01	0.15	0	1
7	Open shrublands	0.01	0.15	0	1
8	Woody savannas	0.01	0.15	0	1
9	Savannas	0.01	0.15	0	1
10	Grasslands	0.01	0.15	0	1
11	Permanent wetlands	-	-	0	1
12	Croplands	0	0	1	0
13	Urban built-up	-	-	0	1
14	Cropland/Natural vegetation mosaic	0.0001	0.05	0.8	0.2
15	Snow and ice	-	-	0	1
16	Barren or sparsely vegetated	0.1	0.5	0	1
254	Unclassified	-	-	0	1
255	Fill Value	-	-	0	1

Table S.10: ESA land cover classification linked with C factor ranges of the respective land cover and weights to calculate mixed C values for shared landuses of non crop land cover and crops

Value	*Label*	C_{LC}	w_{Crop}	w_{LC}
10	Cropland	0	1	0
11	Crop, herb cover	0.1	0.8	0.2
12	Crop, Tree, shrub cover	0.003	0.8	0.2
20	Crop irrigated or post flood	0	1	0
30	Mosaic cropland (>50%) / natural vegetation (tree, shrub, herbaceous cover) (<50%)	0.0265	0.75	0.25
40	Mosaic natural vegetation (tree, shrub, herbaceous cover) (>50%) / cropland (<50%)	0.0265	0.25	0.75
50	Tree cover, broadleaved, evergreen, closed to open (>15%)	0.0016	0	1
60	Tree cover, broadleaved, deciduous, closed to open (>15%)	0.0016	0	1
61	Tree cover, broadleaved, deciduous, closed (>40%)	4e-04	0	1
62	Tree cover, broadleaved, deciduous, open (15-40%)	0.0027	0	1
70	Tree cover, needleleaved, evergreen, closed to open (>15%)	0.0016	0	1
90	Tree cover, mixed leaf type (broadleaved and needleleaved)	4e-04	0	1
100	Mosaic tree and shrub (>50%) / herbaceous cover (<50%)	0.08	0	1
110	Mosaic herbaceous cover (>50%) / tree and shrub (<50%)	0.08	0	1
120	Shrubland	0.08	0	1
122	Deciduous shrubland	0.08	0	1
130	Grassland	0.08	0	1
150	Sparse vegetation (tree, shrub, herbaceous cover) (<15%)	0.3	0	1
152	Sparse shrub (<15%)	0.3	0	1
153	Sparse herbaceous cover (<15%)	0.4	0	1
160	Tree cover, flooded, fresh or brakish water	0.003	0	1
170	Tree cover, flooded, saline water	0.003	0	1
180	Shrub or herbaceous cover, flooded, fresh/saline/brakish water	0.15	0	1
190	Urban areas	0	0	1
200	Bare areas	0.5	0	1
201	Consolidated bare areas	0.15	0	1
202	Unconsolidated bare areas	0.5	0	1

S.2 USLE model input factors - Summary statistics for individual realizations

This section summarizes the individual realizations for the four analyzed USLE input factors to give a general overview. The following tables show quantile values of the USLE input realizations analyzed for the entire study area of Uganda and Kenya.

Table S.11: Summary statistics for the R factor realizations

Quantile	R_{Roose}	R_{Moore}	R_{Lo}	R_{Renard}	R_{Nakil}	$R_{Fenta,P}$	$R_{Fenta,MFI}$	R_{TMPA}	$R_{GloREDa}$
min	1298	52.54	560.5	154	946.1	0	359.6	1.221	857.2
q.25	3953	1774	1629	925.6	1210	1193	1796	2774	1943
median	6851	3652	2795	2243	1581	2696	2668	3956	3432
q.75	9636	5458	3915	4324	2046	3897	3306	5463	4801
max	22741	13952	9187	25755	6875	9099	11982	31068	12930

Table S.12: Summary statistics for the K factor realizations

Quantile	$K_{Soilgr.,Wischm.}$	$K_{Soilgr.,Will.}$	$K_{Soilgr.,Torri}$	$K_{GSDE,Wischm.}$	$K_{GSDE,Will.}$	$K_{GSDE,Torri}$
min	0.004999	0.01077	0.001	1e-04	0.007642	1e-04
q.25	0.01711	0.02284	0.07642	0.01416	0.02318	0.0753
median	0.01931	0.02465	0.07997	0.01867	0.02738	0.08232
q.75	0.0218	0.02696	0.08422	0.02576	0.03165	0.09243
max	0.03798	0.03933	0.109	0.05513	0.05214	0.1484

Table S.13: Summary statistics for the LS factor realizations

Quantile	$LS_{SRTM,Moore}$	$LS_{SRTM,Desmet}$	$LS_{SRTM,Boehner}$	$LS_{ASTERMoore}$	$LS_{ASTER,Desmet}$	$LS_{ASTER,Boehner}$
min	0	0.03	0	0	0.03	0
q.25	0	0.1249	0	0	0.3187	0.06382
median	0.01319	0.334	0.07447	0.1963	0.8278	0.1494
q.75	0.3196	0.9901	0.2377	0.8331	1.879	0.5966
max	91.48	19.31	70.63	226.6	19.75	212.7

Table S.14: Summary statistics for the C factor realizations

Quantile	$C_{NDVI,annual}$	$C_{NDVI,rainy}$	$C_{ESA,admin.}$	$C_{ESA,Monfr.}$	$C_{MODIS_admin.}$	$C_{MODIS,Monfr.}$
min	8.715e-07	5.874e-07	0	0	0	0
q.25	0.0591	0.04719	0.08	0.08	0.1498	0.1499
median	0.2137	0.1749	0.08	0.08	0.15	0.15
q.75	0.4019	0.3546	0.15	0.232	0.15	0.15
max	1	1	0.5	0.5	0.5	0.5

S.3 Issues with LS factor calculation with ASTER DEM

As outlined in the main document of this work, the realizations for the LS factor that used ASTER DEM (NASA/METI/AIST/Japan Spacesystems, and U.S./Japan ASTER Science Team, 2009) for their computation were excluded from the analyses as issues were encountered in the simulation results that stem from noise and artefacts in the ASTER DEM inout data. As a result, only three instead of six realizations for the LS factor were used. Fig. S1 shows the LS factor realizations that result from SRTM 90m (Jarvis et al., 2008) and ASTER DEM when employing the method of Desmet and Govers (1996) for the LS calculation. The panels a) and b) show the results for the entire study area. The panels c) and d) show the detail located in the North-East of Kenya. While the LS calculations using the SRTM show low values close to 0 for large regions where the terrain is overall flat, the LS realization that implemented the ASTER DEM shows (i) random, non-systematic noise (the yellow scatters in flat terrain with no noteworthy heterogeneity in landscape) and (ii) systematic errors (strips), which originate from satellite malfunction or issues in data processing. (i) and (ii) can be clearly seen in the detail showing the dry, north-eastern part of Kenya. Based on the identified noise patterns (among other patterns e.g. in northern Uganda, that are not shown in detail here) we decided to exclude the LS realizations that are based on the ASTER DEM from the set of LS realizations that were used in the analyses of the manuscript. Although not illustrated here, other methods to calculate the LS factor showed comparable results and supported the assumption that the visible errors result from the input DEM rather than from the computation method itself.

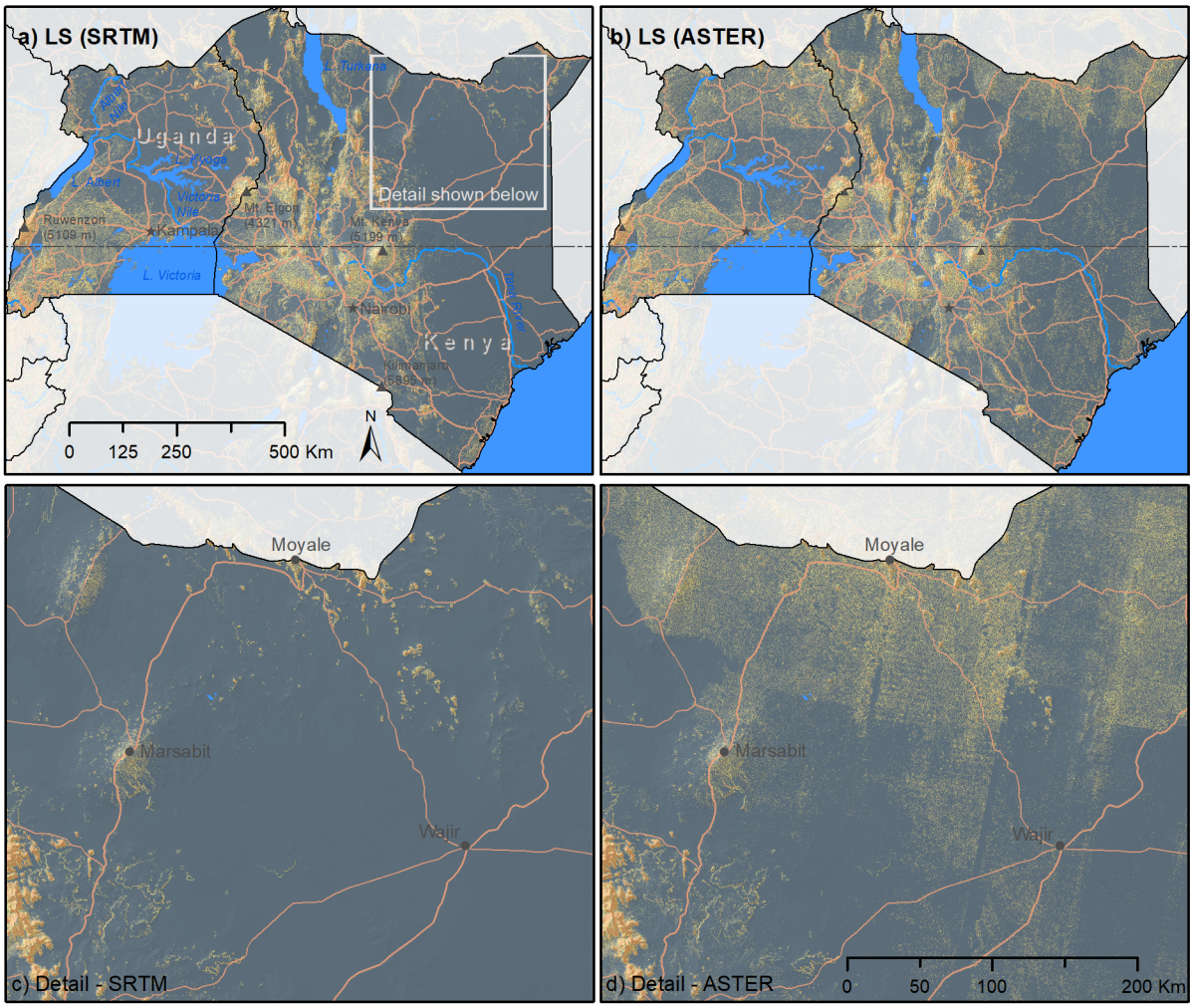

Figure S.1: LS factor realizations that result from SRTM 90m (Jarvis et al., 2008) a) and ASTER DEM (NASA/METI/AIST/Japan Spacesystems, and U.S./Japan ASTER Science Team, 2009) b) when employing the method of Desmet and Govers (1996) for the LS calculation. The map detail indicated in panel a) is shown for SRTM 90m and ASTER DEM in the panels c) and d), respectively. ASTER based calculations show random and systematic noise in the detail in panel d).

S.4 Results for mean *C* values on district level

Implementing the crop shares from the agricultural surveys in Kenya (KNBS, 2015) and Uganda (UBOS, 2010) we calculated average *C* factor values on district level employing the approach described in the previous section. The tables S.15 and S.16 summarise the calculated mean *C* values for the districts of Kenya and Uganda, respectively.

Table S.15: Mean C factor values on district level for Kenya

District	C_{mean}
Baringo	0.338
Bomet	0.315
Bungoma	0.339
Busia	0.332
Elgeyo-Marakwet	0.339
Embu	0.313
Garissa	0.226
Homa Bay	0.338
Isiolo	0.325
Kajiado	0.344
Kakamega	0.335
Kericho	0.357
Kiambu	0.358
Kilifi	0.288
Kirinyaga	0.325
Kisii	0.351
Kisumu	0.317
Kitui	0.33
Kwale	0.375
Laikipia	0.344
Lamu	0.293
Machakos	0.339
Makueni	0.344
Mandera	0.302
Marsabit	0.355
Meru	0.317
Migori	0.347
Mombasa	0
Murang'a	0.343
Nairobi	0.358
Nakuru	0.326
Nandi	0.359
Narok	0.297
Nithi	0.343
Nyamira	0.333
Nyandarua	0.333
Nyeri	0.288

District	C_{mean}
Samburu	0.337
Siaya	0.355
Taita Taveta	0.331
Tana River	0.295
Trans-Nzoia	0.359
Turkana	0.266
Uasin Gishu	0.339
Vihiga	0.349
Wajir	0.28
West Pokot	0.354

Table S.16: Mean C factor values on district level for Uganda

District	C_{mean}
Abim	0.187
Adjumani	0.092
Amolatar	0.138
Amuria	0.148
Amuru	0.14
Apac	0.106
Arua	0.06
Budaka	0.104
Bududa	0.136
Bugiri	0.17
Bukedea	0.089
Bukwo	0.308
Buliisa	0.025
Bundibugyo	0.108
Bushenyi	0.151
Busia	0.113
Butaleja	0.119
Dokolo	0.135
Gulu	0.182
Hoima	0.095
Ibanda	0.156
Iganga	0.101
Isingiro	0.156
Jinja	0.122
Kaabong	0.262
Kabale	0.171
Kabarole	0.145
Kaberamaido	0.131
Kalangala	0.02
Kaliro	0.158
Kampala	0.127

District	C_{mean}
Kamuli	0.123
Kamwenge	0.164
Kanungu	0.178
Kapchorwa	0.182
Kasese	0.12
Katakwi	0.153
Kayunga	0.116
Kibaale	0.171
Kiboga	0.186
Kiruhura	0.154
Kisoro	0.197
Kitgum	0.228
Koboko	0.117
Kotido	0.26
Kumi	0.099
Kyenjojo	0.157
Lira	0.218
Luwero	0.113
Lyantonde	0.16
Manafwa	0.178
Masaka	0.145
Masindi	0.191
Mayuge	0.131
Mbale	0.148
Mbarara	0.152
Mityana	0.171
Moroto	0.248
Moyo	0.163
Mpigi	0.149
Mubende	0.175
Mukono	0.123
Nakapiripirit	0.246
Nakaseke	0.158
Nakasongola	0.06
Namutumba	0.107
Nebbi	0.041
Ntungamo	0.173
Nyadri	0.079
Oyam	0.146
Pader	0.239
Pallisa	0.128
Rakai	0.161
Rukungiri	0.174
Sironko	0.16
Soroti	0.074
Ssembabule	0.164

District	C_{mean}
Tororo	0.046
Wakiso	0.114
Yumbe	0.113

S.5 Results for soil loss on district level

In this work the soil loss estimates that resulted from the USLE model ensemble was averaged on district level for all districts of Kenya and Uganda. In the main document only selected erosion prone districts were selected and analyzed with more detail. In the following we summarize the soil loss estimates for all districts of Kenya (Table S.17) and Uganda (Table S.18).

Table S.17: Quantiles of mean soil loss estimates for all Kenyan districts based on the 972 USLE model setups in $tha^{-1}yr^{-1}$

District	A_{min}	$A_{0.025}$	$A_{0.25}$	A_{median}	A_{mean}	$A_{0.75}$	$A_{0.975}$	A_{max}
Baringo	3.8	6.37	14.23	28.5	45.16	52.81	191.96	419.07
Bomet	0.28	0.74	4.66	20.95	46.71	59.13	243.26	535.72
Bungoma	2.24	4.02	14.23	29.4	53.83	68.77	253.74	478.27
Busia	0.14	0.37	2.13	5.76	13.27	14.42	84.66	176.16
Busia	0.42	1.01	5.98	16.68	34.26	46.3	187.06	326.36
Elgeyo-Marakwet	2.21	4.15	20.54	47.21	85.2	110.6	381.12	797.47
Embu	1.43	3.49	11.85	24.3	45.26	55.41	216.03	398.7
Garissa	0.04	0.09	0.29	0.62	1.22	1.43	6.07	13.26
Homa Bay	1.27	2.96	12.98	25.4	49.39	64.17	241.87	460.75
Isiolo	0.31	0.46	1.35	2.7	5.11	5.79	24.15	58.87
Kajiado	1.03	1.47	3.89	7.68	12.98	15.6	55.57	138.84
Kakamega	0.57	1.32	7.71	20.23	42.55	53.18	229.32	423.42
Kericho	0.77	1.75	11.35	40.34	85.99	112.63	445.07	880.44
Kiambu	1.62	3.1	8.47	17.06	33.22	41.06	148.06	374.2
Kilifi	0.71	1.1	2.59	5.21	8.55	9.96	37.07	76.14
Kirinyaga	1.7	3.44	10.73	19.94	32.15	39.14	130.04	311.77
Kisii	0.45	1.4	11.03	41.69	87.38	112.13	478.9	855.23
Kisumu	0.77	1.67	8.2	18.87	36.78	48.58	179.19	312.46
Kitui	1.13	1.82	4.82	8.97	15.76	20.05	77.05	120.3
Kwale	1.08	1.74	4.26	8.38	14.26	16.58	65.69	131.82
Laikipia	1.67	2.7	5.78	12.16	19.15	22.38	77.39	154.36
Lamu	0.16	0.27	0.67	1.28	2.21	2.65	10.33	28.36
Machakos	2.21	3.27	8.91	17.72	29.72	36.16	140.89	268.93
Makueni	2.18	3.42	8.82	16.8	28.63	35.4	135.48	257.18
Mandera	0.15	0.28	0.89	1.98	4.08	4.67	18.59	52.47
Marsabit	0.24	0.44	1.39	3.23	6.21	6.98	28.61	77.57
Meru	4.35	6.23	15.49	29.6	47.43	55.31	208.95	381.88
Migori	0.72	1.83	8.79	20.35	40.86	52.09	207.99	401.34

District	A_{min}	$A_{0.025}$	$A_{0.25}$	A_{median}	A_{mean}	$A_{0.75}$	$A_{0.975}$	A_{max}
Mombasa	0.24	0.53	2.85	5.82	11.92	14.11	56.94	144.75
Murang'a	0.91	2.4	13.75	32.42	64.47	74.91	298.77	736.36
Nairobi	0.6	0.99	2.49	4.96	8.19	9.67	30.22	62.62
Nakuru	1.98	3.55	10.32	19.15	34.75	42.17	137.92	327.17
Nandi	0.8	1.67	10.92	44.57	95.42	123.65	501.74	1044.62
Narok	1.94	3.8	9.94	18.79	31.77	38.16	122.35	278.61
Nithi	0.88	2.12	9.61	21.72	41.55	50.02	216.83	401.98
Nyamira	0.36	1.01	7.94	46.09	100.58	129.21	553.75	1049.56
Nyandarua	1.55	2.96	10.19	20.41	37.28	44.56	161.21	421.7
Nyeri	3.75	4.91	15.23	28.99	49.03	58.68	200.25	509.01
Samburu	2.93	4.28	11.13	21.12	35.95	43.86	149.83	364.36
Siaya	0.42	0.93	5.42	14.69	30.4	38.9	161.58	289.34
Taita Taveta	1.22	1.85	4.32	8.38	13.9	17.05	53.06	98.17
Tana River	0.12	0.2	0.57	1.14	2.21	2.55	10.38	26.09
Trans-Nzoia	1.06	2.24	8.36	17.34	32.72	41.69	135.38	317.96
Turkana	0.63	1.16	4.21	8.84	17.56	20.1	87.18	235.97
Uasin Gishu	0.45	1.32	5.04	11.16	20.91	26.36	92.86	194.55
Vihiga	1.01	2.43	14.82	42.74	90.58	116.79	490.03	894.4
Wajir	0.05	0.1	0.36	0.84	1.7	2.01	7.96	22.51
West Pokot	5.7	8.19	19.57	38.27	62.83	74.23	282.83	658.77

Table S.18: Quantiles of mean soil loss estimates for all Ugandan districts based on the 972 USLE model setups in $tha^{-1}yr^{-1}$

District	A_{min}	$A_{0.025}$	$A_{0.25}$	A_{median}	A_{mean}	$A_{0.75}$	$A_{0.975}$	A_{max}
Abim	0.45	0.87	3.77	9.32	19.57	20.93	111.83	266.39
Adjumani	0.17	0.4	1.39	3.54	8.27	8.56	51.3	135.02
Amolatar	0.14	0.32	1	1.96	3.81	4.45	20.53	47.31
Amuria	0.32	0.48	1.34	2.74	4.6	5.56	20.97	47.91
Amuru	0.25	0.61	2.15	4.73	9.51	11.26	51.36	125.75
Apac	0.11	0.25	1.1	2.45	5.38	6.17	32.21	71.53
Arua	0.52	1.09	3.48	7.76	15.51	18.14	87.64	218.54
Budaka	0.26	0.51	1.53	3.46	6.72	7.55	36.1	83.14
Bududa	7.2	16.99	48.59	90.69	138.78	173.71	544.75	1080.05
Bugiri	0.18	0.44	2.18	5.8	12.62	15.63	72.79	144.78
Bukedea	0.29	0.4	1.07	2.54	4.65	5.62	24.03	57.89
Bukwo	4.01	6.71	18.91	40.58	71.78	83.36	346.17	862.47
Buliisa	0.34	0.69	1.8	3.63	6.62	7.74	32.8	81.8
Bundibugyo	2.77	4.81	11.56	22.82	35.2	42.36	149.53	351.58

District	A_{min}	$A_{0.025}$	$A_{0.25}$	A_{median}	A_{mean}	$A_{0.75}$	$A_{0.975}$	A_{max}
Bushenyi	0.83	1.62	8.15	21.92	45.47	55.09	234.39	581.16
Busia	0.14	0.37	2.13	5.76	13.27	14.42	84.66	176.16
Busia	0.42	1.01	5.98	16.68	34.26	46.3	187.06	326.36
Butaleja	0.09	0.22	1.05	2.32	4.94	5.46	26.27	70.94
Dokolo	0.23	0.49	1.65	3.26	6.56	7.63	36.51	82.59
Gulu	0.17	0.43	1.56	3.66	7.27	8.25	43.18	94.47
Hoima	0.38	0.86	3.58	8.73	18.36	20.3	107.23	263.87
Ibanda	0.56	1.18	7.3	22.89	48.91	61.11	255.55	638.36
Iganga	0.1	0.25	1.47	4.19	10.02	10.68	58.44	141.16
Isingiro	1.31	2.96	10.81	21.64	39.31	48.51	176.13	440.66
Jinja	0.35	0.77	3.83	10.23	21.65	25.05	122.2	260.94
Kaabong	1.35	2.08	7.9	15.31	30.26	35.03	140.63	417.29
Kabale	6.33	11.42	38.18	75.16	139.47	168.4	591.69	1528.61
Kabarole	3.51	5.83	17.44	31.97	58.4	71.15	252.52	679.17
Kaberamaido	0.15	0.34	1.37	2.65	5.67	6.57	32.23	72.59
Kalangala	0.44	0.83	2.37	4.56	7.47	9.24	29.94	77.59
Kaliro	0.19	0.43	1.59	3.09	6.62	7.83	37.97	76.33
Kampala	0.36	0.9	2.84	5.78	10.47	12.18	48.75	134.17
Kamuli	0.13	0.31	1.32	3.13	6.88	7.94	38.47	94.85
Kamwenge	0.24	0.52	3.37	11.81	26.91	34.51	142.76	362.28
Kanungu	1.03	2.17	11.96	29.16	58.95	72.99	281.56	716.8
Kapchorwa	3.73	5.72	18.18	35.99	59.51	69.22	273.16	683.5
Kasese	5.87	9.7	28.24	54.78	100.06	116.5	462.94	1456
Katakwi	0.15	0.31	0.84	1.73	2.85	3.37	12.85	31.6
Kayunga	0.06	0.14	0.75	2.66	6.36	7.38	36.85	95.09
Kibaale	0.12	0.27	1.84	12.02	27.74	34.26	154.96	440.75
Kiboga	0.11	0.25	1.79	7.42	16.46	21.55	85.2	184.72
Kiruhura	0.28	0.6	3.51	7.98	17.86	21.22	93.63	219.21
Kisoro	4.17	7.66	26.4	55.33	104.63	123.9	502.82	1176.19
Kitgum	0.35	0.63	2.1	5.31	11.36	12.15	66.64	175.6
Koboko	0.5	1.14	4.08	8.58	17.76	21.09	96.81	255.96
Kotido	0.26	0.43	1.3	2.44	4.67	5.45	20.23	54.87
Kumi	0.38	0.49	1.39	3.16	5.5	6.76	26.77	61.62
Kyenjojo	0.08	0.21	1.53	12.67	29.33	37.14	156.18	408.83
Lira	0.25	0.58	2.01	3.76	7.04	8.96	33.35	68.17
Luwero	0.05	0.1	0.65	4.44	10.47	12.61	61.59	143.92
Lyantonde	0.45	1.05	4.76	10.64	21.62	24.96	113.22	280.43
Manafwa	2.82	6.27	21.94	43.16	75.25	92.97	334.56	784.16
Masaka	0.43	0.9	4.4	10.18	20.53	24.71	100.07	222.03
Masindi	0.11	0.28	1.56	4.62	10.04	12.67	54.43	118.38
Mayuge	0.24	0.6	2.76	7.64	16.94	19.9	96.49	224.54
Mbale	0.8	1.86	8.88	20.37	39.45	47.56	192.09	491.53
Mbarara	1.17	2.4	10.83	22.35	44.29	53.06	216.08	537.82
Mityana	0.11	0.24	1.38	13.11	29.6	37.63	163.1	421.42
Moroto	0.34	0.54	2.61	6.22	12.15	14.5	54.41	143.37
Moyo	0.75	1.54	5	11.57	23.45	25.48	128.32	348.41

District	A_{min}	$A_{0.025}$	$A_{0.25}$	A_{median}	A_{mean}	$A_{0.75}$	$A_{0.975}$	A_{max}
Mpigi	0.17	0.4	2.48	9.51	21.05	26.32	117.76	266.3
Mubende	0.13	0.32	2.34	14.12	32.39	40.82	179.79	483.67
Mukono	0.25	0.57	2.87	9.73	22.68	27.35	135.69	283.77
Nakapiripirit	0.61	1.18	3.43	6.65	12.36	15.37	53.39	131.04
Nakaseke	0.08	0.16	1	3.06	6.69	8.38	37.5	82.68
Nakasongola	0.11	0.18	0.59	1.34	2.93	3.24	14.96	49.23
Namutumba	0.19	0.42	1.6	3.61	7.82	8.27	46.96	98.26
Nebbi	0.72	1.42	4.41	10.73	21.97	23.54	130.48	320.27
Ntungamo	1.55	3.24	13.54	27.23	51.78	63.08	233.03	589.4
Nyadri	0.69	1.33	4.36	9.5	17.84	20.65	89.71	245.9
Oyam	0.1	0.22	1.19	2.95	6.65	7.86	36.78	85.58
Pader	0.16	0.32	1.23	3.19	6.52	6.5	40.92	91.25
Pallisa	0.25	0.51	1.56	3.25	6.15	7.1	31.89	75.11
Rakai	0.83	1.59	6.37	13.15	25.6	30.5	127.61	289.09
Rukungiri	0.87	1.7	9.16	23.16	47.04	56.62	226.57	555.65
Sironko	3.02	5.88	17.71	34.32	54.44	68.44	214.86	512.23
Soroti	0.27	0.43	1.23	2.96	5.43	6.18	31.19	67.77
Ssembabule	0.18	0.45	2.94	7.78	16.82	19.53	89.37	226.69
Tororo	0.3	0.49	1.61	4.46	10.21	10.28	69.82	152
Wakiso	0.36	0.75	3.77	9.96	22.18	25.48	128.6	283.77
Yumbe	0.26	0.64	2.12	4.44	8.68	10.26	43.56	129.48

The distributions of the mean soil losses that resulted from all 972 USLE model realizations are additionally plotted for the districts of Kenya and Uganda in the figures S.2 and S.3.

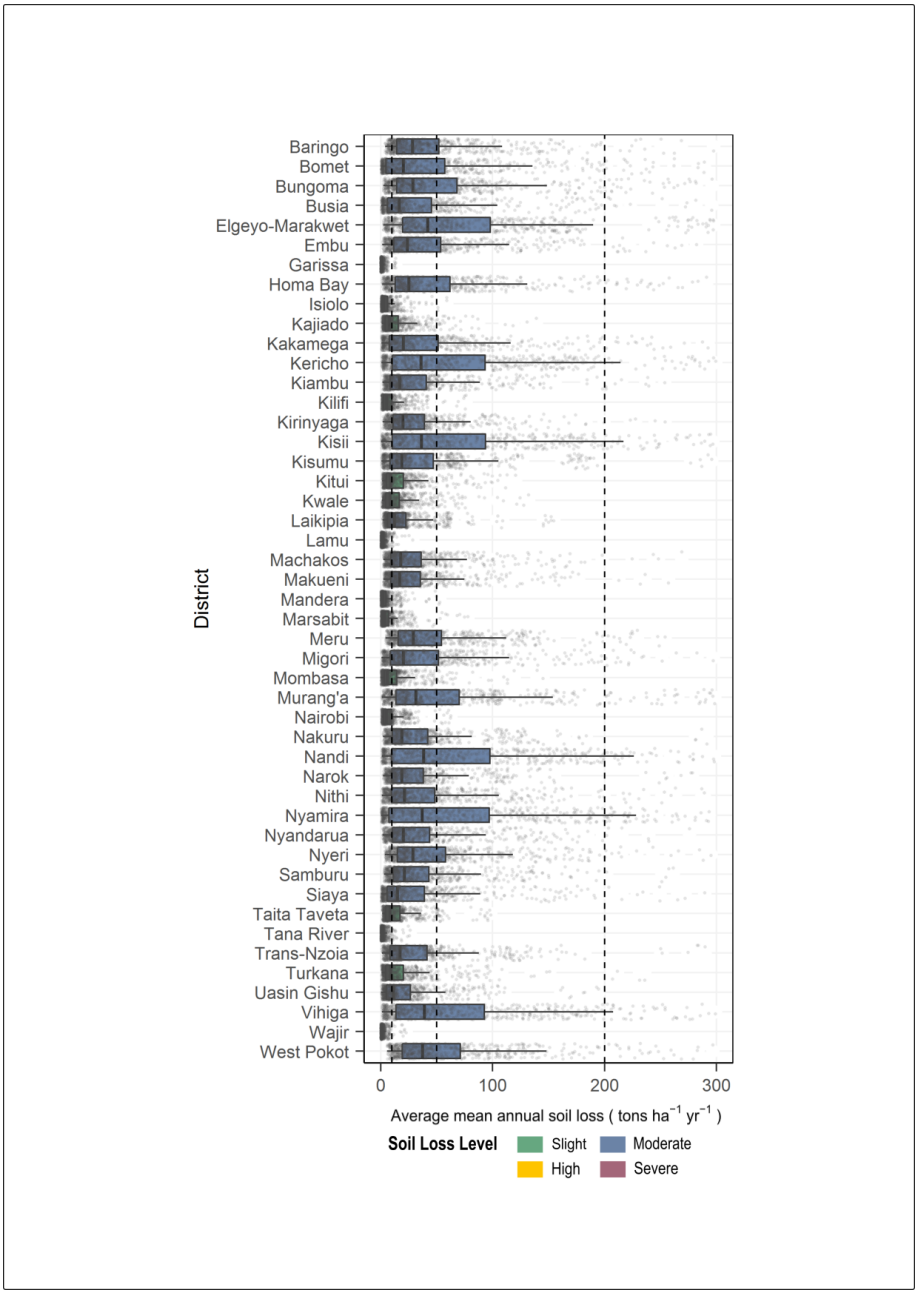

Figure S.2: Mean soil loss in the districts of Kenya. The grey dots show the estimated soil losses from all 972 USLE realizations. The boxplots represent the quantiles for the district results.

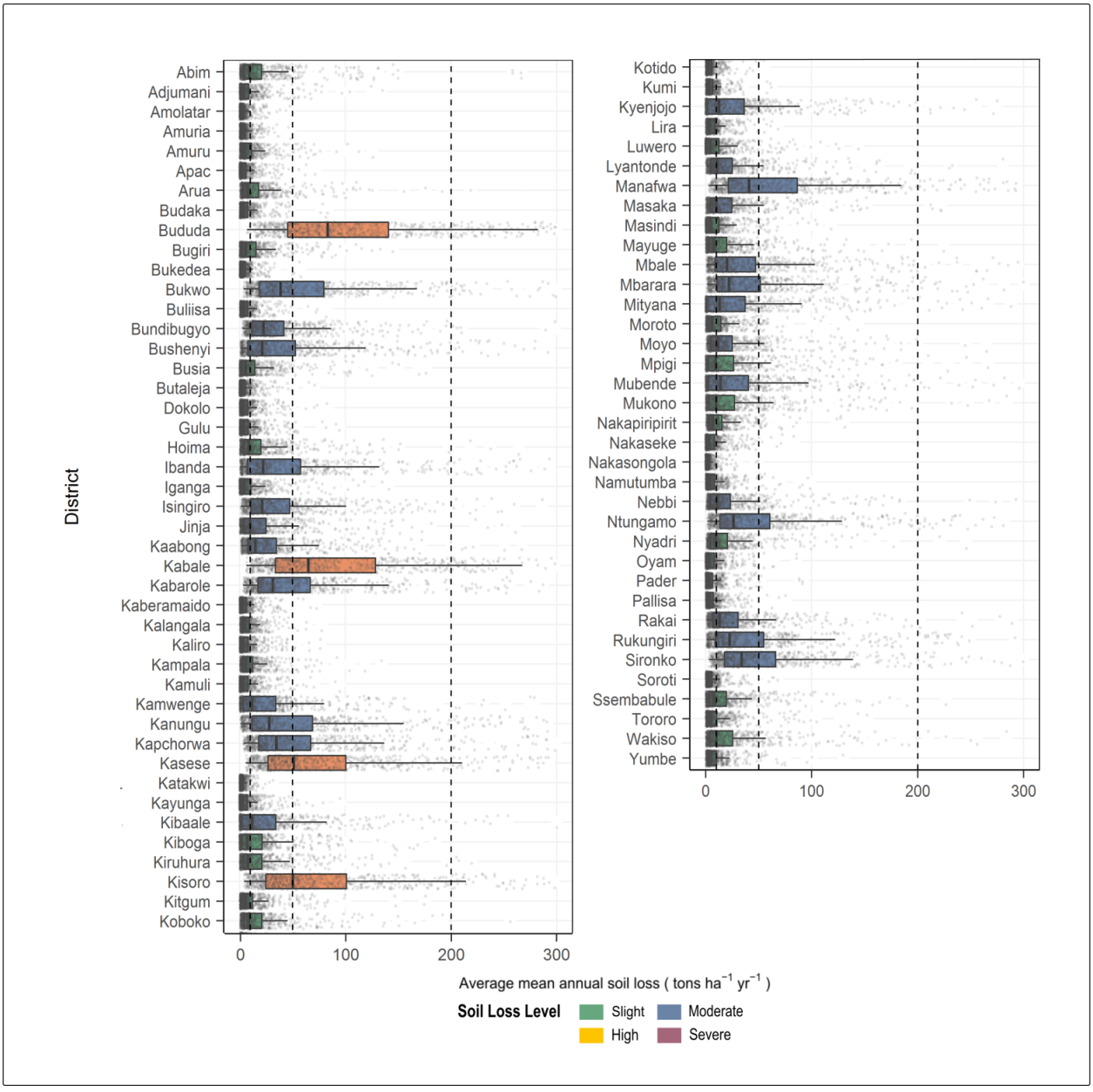

Figure S.3: Mean soil loss in the districts of Uganda. The grey dots show the estimated soil losses from all 972 USLE realizations. The boxplots represent the quantiles for the district results.

S.6 Sensitivity of soil loss estimates to individual input factors

Fig. 7 in the main document illustrates the spatial distribution of the most important USLE input factors for the computation of the soil loss. Fig. S4 shows the indvidual results for the sensitivity index for all four USLE inputs that were analyzed. The dominant patterns that are also visible in Fig. 7 are also shown by the individual results. While particularly the C factor shows large values in the highly vegetated areas in Uganda, patterns ther result from the soil input data are visible for the K factor in the dry regions of northern Kenya. The LS factor shows highly hetrogenious patterns in the entire study area that is also visible in Fig. 7. Although the R factor shows an overall high sensitivity and a low variability for the entire study region it is not as sensitive as other inputs and thus identified as the most dominant input in Fig. 7.

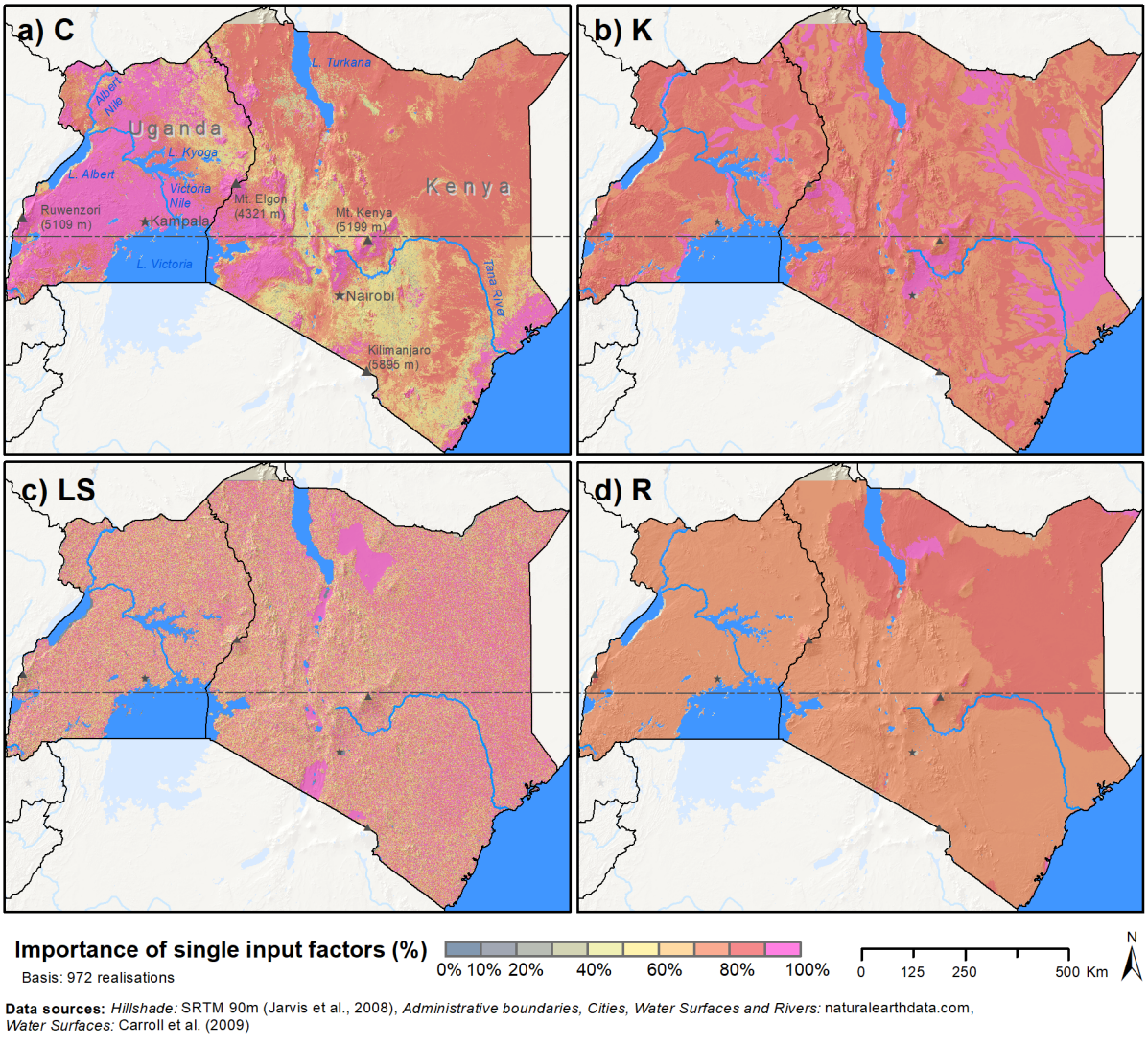

Figure S.4: Results for the sensitivity index calculated for all four USLE input factors.

References

Angima, S. D., Stott, D. E., O'Neill, M. K., Ong, C. K. and Weesies, G. A.: Soil erosion prediction using RUSLE for central Kenyan highland conditions, Agriculture, Ecosystems and Environment, 97(1-3), 295–308, doi:10.1016/S0167-8809(03)00011-2, 2003.

Arnoldus, H. M. J.: An approximation of the rainfall factor in the Universal Soil Loss Equation., in Assessment of erosion, edited by M. De Boodt and D. Gabriels, pp. 127–132, John Wiley & Sons, Ltd., Chichester, UK., 1980.

Baruth, B., Genovese, G. and Montanarella, L., Eds.: Pedo-transfer rule 5 (PTR05): top soil structure class (STS), in New soil information for the mars crop yield forecasting system, European Commission, Joint Research Centre (EC JRC). [online] Available from: https://esdac.jrc.ec.europa.eu/Projects/SINFO/pdf/annex4_5.pdf, 2006.

Borrelli, P., Robinson, D. A., Fleischer, L. R., Lugato, E., Ballabio, C., Alewell, C., Meusburger, K., Modugno, S., Schütt, B., Ferro, V., Bagarello, V., Oost, K. V., Montanarella, L. and Panagos, P.: An assessment of the global impact of 21st century land use change on soil erosion, Nature Communications, 8(1), doi:10.1038/s41467-017-02142-7, 2017.

Bosco, C., De Rigo, D., Dewitte, O., Poesen, J. and Panagos, P.: Modelling soil erosion at European scale: Towards harmonization and reproducibility, Natural Hazards and Earth System Sciences, 15(2), 225–245, doi:10.5194/nhess-15-225-2015, 2015.

Böhner, J. and Selige, T.: Spatial prediction of soil attributes using terrain analysis and climate regionalisation, in 'SAGA - analysis and modelling applications', edited by J. Böhner, K. McCloy, and J. Strobl, Göttinger Geographische Abhandlungen, Göttingen, 13-28., 2006.

Channan, S., Collins, K. and Emanuel, W. R.: Global mosaics of the standard MODIS land cover type data, 2014.

Conrad, O., Bechtel, B., Bock, M., Dietrich, H., Fischer, E., Gerlitz, L., Wehberg, J., Wichmann, V. and Böhner, J.: System for automated geoscientific analyses (SAGA) v. 2.1.4, Geoscientific Model Development, 8(7), 1991–2007, doi:10.5194/gmd-8-1991-2015, 2015.

Desmet, P. and Govers, G.: A gis procedure for automatically calculating the usle ls factor on topographically complex landscape units, Journal of soil and water conservation, 51(5), 427–433, 1996.

Didan, K.: MOD13Q1 modis/terra vegetation indices 16-day l3 global 250m sin grid v006, NASA EOSDIS Land Processes DAAC, doi:10.5067/MODIS/MOD13Q1.006, 2015.

ESA: ESA land cover climate change initiative (esa lc cci), via centre for environmental data analysis, [online] Available from: http://maps.elie.ucl.ac.be/CCI, 2017.

ESRI: ArcGIS Desktop: Release 10.1, 2012.

Fenta, A. A., Yasuda, H., Shimizu, K., Haregeweyn, N., Kawai, T., Sultan, D., Ebabu, K. and Belay, A. S.: Spatial distribution and temporal trends of rainfall and erosivity in the eastern africa region, Hydrological Processes, 31(25), 4555–4567, doi:10.1002/hyp.11378, 2017.

Fenta, A. A., Tsunekawa, A., Haregeweyn, N., Poesen, J., Tsubo, M., Borrelli, P., Panagos, P., Vanmaercke, M., Broeckx, J., Yasuda, H., Kawai, T. and Kurosaki, Y.: Land susceptibility to water and wind erosion risks in the east africa region, Science of The Total Environment, 703, 135016, doi:10.1016/j.scitotenv.2019.135016, 2020.

Ferro, V., Giordano, G. and Iovino, M.: Isoerosivity and erosion risk map for sicily, Hydrological Sciences Journal, 36(6), 549–564, doi:10.1080/02626669109492543, 1991.

Fick, S. E. and Hijmans, R. J.: WorldClim 2: new 1-km spatial resolution climate surfaces for global land areas, International Journal of Climatology, 37(12), 4302–4315, doi:10.1002/joc.5086, 2017.

Freeman, T.: Calculating catchment area with divergent flow based on a regular grid, Computers & Geosciences, 17(3), 413–422, doi:10.1016/0098-3004(91)90048-i, 1991.

Hengl, T., De Jesus, J. M., Heuvelink, G. B., Gonzalez, M. R., Kilibarda, M., Blagotić, A., Shangguan, W., Wright, M. N., Geng, X., Bauer-Marschallinger, B., Guevara, M. A., Vargas, R., MacMillan, R. A., Batjes, N. H., Leenaars, J. G., Ribeiro, E., Wheeler, I., Mantel, S. and Kempen, B.: SoilGrids250m: Global gridded soil information based on machine learning, PLoS ONE, 12(2), 1–40, doi:10.1371/journal.pone.0169748, 2017.

Jarvis, A., Reuter, H. I., Nelson, A. and Guevara, E.: Hole-filled srtm for the globe version 4. [online] Available from: https://cgiarcsi.community/data/srtm-90m-digital-elevation-database-v4-1/, 2008.

Karamage, F., Zhang, C., Liu, T., Maganda, A. and Isabwe, A.: Soil erosion risk assessment in Uganda, Forests, 8(2), 52, doi:10.3390/f8020052, 2017.

KNBS: Section agriculture, in County statistical abstracts, Kenya National Bureau of Statistics, Nairobi, Kenya., 2015.

Lo, A., El-Swaify, S. A., Dangler, E. W. and Shinshiro, L.: Effectiveness of EI30 as an erosivity index in Hawaii, in Soil erosion and conservation, edited by S. A. El-Swaify, W. C. Moldenhauer, and A. Lo, pp. 384–392, Soil Conservation Society of America, Ankeny, IA, USA., 1985.

Monfreda, C., Ramankutty, N. and Foley, J. A.: Farming the planet: 2. Geographic distribution of crop areas, yields, physiological types, and net primary production in the year 2000, Global Biogeochemical Cycles, 22(1), 1–19, doi:10.1029/2007GB002947, 2008.

Moore, I. D., Grayson, R. B. and Ladson, A. R.: Digital terrain modelling: A review of hydrological, geomorphological, and biological applications, Hydrological Processes, 5(1), 3–30, doi:10.1002/hyp.3360050103, 1991.

Moore, T. R.: Rainfall Erosivity in East Africa, Geografiska Annaler. Series A, Physical Geography, 61(3/4), 147–156, doi:10.2307/520909, 1979.

Morgan, R. P. C.: Soil erosion and conservation, John Wiley & Sons., 2009.

Naipal, V., Reick, C., Pongratz, J. and Van Oost, K.: Improving the global applicability of the RUSLE model - Adjustment of the topographical and rainfall erosivity factors, Geoscientific Model Development, 8(9), 2893–2913, doi:10.5194/gmd-8-2893-2015, 2015.

Nakil, M.: Analysis of parameters causing water induced soil erosion, in Unpublished fifth annual progress seminar, indian institute of technology, bombay., 2014.

NASA/METI/AIST/Japan Spacesystems, and U.S./Japan ASTER Science Team: ASTER Global Digital Elevation Model., 2009.

Panagos, P., Meusburger, K., Ballabio, C., Borrelli, P. and Alewell, C.: Soil erodibility in Europe: A high-resolution dataset based on LUCAS, Science of the Total Environment, 479-480(1), 189–200, doi:10.1016/j.scitotenv.2014.02.010, 2014.

Panagos, P., Borrelli, P. and Meusburger, K.: A New European Slope Length and Steepness Factor (LS-Factor) for Modeling Soil Erosion by Water, Geosciences, 5(2), 117–126, doi:10.3390/geosciences5020117, 2015a.

Panagos, P., Borrelli, P., Meusburger, K., Alewell, C., Lugato, E. and Montanarella, L.: Estimating the soil erosion cover-management factor at the European scale, Land Use Policy, 48, 38–50, doi:10.1016/j.landusepol.2015.05.021, 2015b.

Panagos, P., Borrelli, P., Poesen, J., Ballabio, C., Lugato, E., Meusburger, K., Montanarella, L. and Alewell, C.: The new assessment of soil loss by water erosion in Europe, Environmental Science and Policy, 54, 438–447, doi:10.1016/j.envsci.2015.08.012, 2015c.

Panagos, P., Borrelli, P., Meusburger, K., Yu, B., Klik, A., Jae Lim, K., Yang, J. E., Ni, J., Miao, C., Chattopadhyay, N., Sadeghi, S. H., Hazbavi, Z., Zabihi, M., Larionov, G. A., Krasnov, S. F., Gorobets, A. V., Levi, Y., Erpul, G., Birkel, C., Hoyos, N., Naipal, V., Oliveira, P. T. S., Bonilla, C. A., Meddi, M., Nel, W., Al Dashti, H., Boni, M., Diodato, N., Van Oost, K., Nearing, M. and Ballabio, C.: Global rainfall erosivity assessment based on high-temporal resolution rainfall records, Scientific Reports, 7(1), 4175, doi:10.1038/s41598-017-04282-8, 2017.

Quinn, P., Beven, K., Chevallier, P. and Planchon, O.: The prediction of hillslope flow paths for distributed hydrological modelling using digital terrain models, Hydrological Processes, 5(1), 59–79, doi:10.1002/hyp.3360050106, 1991.

Renard, K. G. and Freimund, J. R.: Using monthly precipitation data to estimate the R-factor in the revised USLE, Journal of Hydrology, 157(1-4), 287–306, doi:10.1016/0022-1694(94)90110-4, 1994.

Roose, E. J.: Erosion et ruissellement en afrique de l'Ouest : Vingt années de mesures en petites parcelles expérimentales, Office de la scientifique et Technique Outre-Mer, Centre D'Adiopodoumé, Côte d'Ivoire., 1975.

Shangguan, W., Dai, Y., Duan, Q., Liu, B. and Yuan, H.: A global soil data set for earth system modeling, Journal of Advances in Modeling Earth Systems, 6, 249–263, doi:10.1002/2013MS000293, 2014.

Tamene, L. and Le, Q. B.: Estimating soil erosion in sub-Saharan Africa based on landscape similarity mapping and using the revised universal soil loss equation (RUSLE), Nutrient Cycling in Agroecosystems, 102(1), 17–31, doi:10.1007/s10705-015-9674-9, 2015.

Torri, D., Poesen, J. W. A. and Borselli, L.: Predictability and uncertainty of the soil erodibility factor using a global dataset, CATENA, 31, 1–22, doi:https://doi.org/10.1016/S0341-8162(97)00036-2, 1997.

UBOS: Volume IV: Crop Area and Production Report, in Uganda census of agriculture 2008/2009, p. 178, Uganda Bureau of Statistics, Kampala, Uganda., 2010.

Van der Knijff, J., Jones, R. and Montanarella, L.: Soil Erosion Risk Assessment in Europe, EUR 19044 EN., European Soil Bureau, European Comission., 2000.

Vrieling, A., Hoedjes, J. C. B. and Velde, M. van der: Towards large-scale monitoring of soil erosion in Africa: Accounting for the dynamics of rainfall erosivity, Global and Planetary Change, 115, 33–43, doi:10.1016/j.gloplacha.2014.01.009, 2014.

Wang, L. and Liu, H.: An efficient method for identifying and filling surface depressions in digital elevation models for hydrologic analysis and modelling, International Journal of Geographical Information Science, 20(2), 193–213, doi:10.1080/13658810500433453, 2006.

Williams, J. R.: The EPIC model - Soil Erosion, in Computer models of watershed hydrology, edited by V. P. Singh, pp. 909–1000, Water Resources Publications, Highlands Ranch, CO, USA., 1995.

Wischmeier, W. H. and Smith, D. D.: Predicting rainfall erosion losses - a guide to conservation planning., USDA, Hyattsville, Maryland., 1987.

Yang, D., Kanae, S., Oki, T., Koike, T. and Musiake, K.: Global potential soil erosion with reference to land use and climate changes, Hydrological Processes, 17(14), 2913–2928, doi:10.1002/hyp.1441,

2003.

Yu, B. and Rosewell, C.: A robust estimators of the R-factor for the Universal Soil Loss Equation, American Society of Agricultural Engineers, 39(2), 559–561, doi:https://doi.org/10.13031/2013.27535, 1996.

Zevenbergen, L. W. and Thorne, C. R.: Quantitative analysis of land surface topography, Earth Surface Processes and Landforms, 12(1), 47–56, doi:10.1002/esp.3290120107, 1987.